Available online at www.sciencedirect.com

SCIENCE DIRECT

Virology 333 (2005) 301–315

VIROLOGY

www.elsevier.com/locate/yviro

Importance of sequence and structural elements within a viral replication repressor

Jiuchun Zhang, Anne E. Simon*

Department of Cell Biology and Molecular Genetics, 1109 Microbiology Building, University of Maryland, College Park, MD 20742, USA

Received 18 August 2004; received in revised form 17 November 2004; accepted 9 December 2004

Abstract

Efficient replication of plus-strand RNA viruses requires a 3′ proximal core promoter and an increasingly diverse inventory of supporting elements such as enhancers, repressors, and 5′ terminal sequences. While core promoters have been well characterized, much less is known about structure–functional relationships of these supporting elements. Members of the genus *Carmovirus* family *Tombusviridae* contain a hairpin (H5) proximal to the core promoter that functions as a repressor of minus-strand synthesis in vitro through an interaction between its large symmetrical internal loop (LSL) and 3′ terminal bases. *Turnip crinkle virus* satellite RNA satC with the H5 of carmovirus *Japanese iris necrosis virus* or *Cardamine chlorotic fleck virus* (CCFV) did not accumulate to detectable levels even though 3′ end base-pairing would be maintained. Replacement of portions of the satC H5 with analogous portions from CCFV revealed that the cognate LSL and lower stem were of greater importance for satC accumulation than the upper stem. In vivo selex of the H5 upper stem and terminal GNRA tetraloop revealed considerable plasticity in the upper stem, including the presence of three- to six-base terminal loops, allowed for H5 function. In vivo selex of the lower stem revealed that both a stable stem and specific base pairs contributed to satC fitness. Surprisingly, mutations in H5 had a disproportionate effect on plus-strand accumulation that was unrelated to the stability of the mutant plus-strands. In addition, fitness to accumulate in plants did not always correlate with enhanced ability to accumulate in protoplasts, suggesting that H5 may be multifunctional.

Keywords: Plus-strand RNA virus; *Carmovirus*; Tombusviridae

Introduction

Replication of all plus-strand RNA viruses requires a multistep process that begins with reiterative copying of the infecting genome to generate complementary minus-sense intermediates, followed by reiterative copying of the intermediates to generate progeny plus-strand RNAs. This process requires that the viral-encoded RNA-dependent RNA polymerase (RdRp) locate the 3′ end of its cognate RNA for de novo or primer-dependent initiation of RNA synthesis (Buck, 1996; Kao et al., 2001; van Dijk et al., 2004). Using a reductionist approach, core promoters for minus-strand synthesis have been identified for many plus-strand viruses (Chapman and Kao, 1999; Panavas et al., 2002; Sivakumaran et al., 1999; Song and Simon, 1995; Turner and Buck, 1999). Core promoters generally consist of one or a few 3′ proximal hairpins (Dreher, 1999; Duggal et al., 1994) that can contain multiple sequence and structural features necessary for efficient RdRp recognition (Kim et al., 2000). Promoter elements that specifically interact with the polymerase for initiation of minus-strand synthesis are generally located proximal to 3′ terminal sequences and usually comprise one or more hairpins with adjoining single-stranded sequence (Dreher, 1999). The ability of some viral RNAs to replicate in the absence of large 3′ or 5′ terminal fragments (Todd et al., 1997; Wu and White, 1998) also suggests that, for some virus–host combinations, promoter sequences may be redundant or that additional factors such as close proximity between polymerase and template in replication organelles can obviate the need for distinct molecular recognition (Brown et al., 2004).

While core promoters permit basal levels of RNA transcription, efficient RNA synthesis requires additional

* Corresponding author. Fax: +1 301 314 7930.
E-mail address: Anne_Simon@umail.umd.edu (A.E. Simon).

0042-6822/$ - see front matter © 2005 Elsevier Inc. All rights reserved.
doi:10.1016/j.virol.2004.12.015

viral elements such as structures and sequences at the 5′ ends that may be required for genome circularization (Frolov et al., 2001; Herold and Andino, 2001; Isken et al., 2003; Khromykh et al., 2001; You et al., 2001) and internal elements such as repressors, enhancers, and RNA chaperones, which function either in cis (Barton et al., 2001; Herold and Andino, 2001; Khromykh et al., 2001; Klovins et al., 1998; Murray et al., 2004; Nagy et al., 1999, 2001; Panavas and Nagy, 2003; Pogany et al., 2003; Quadt et al., 1995; Ray and White, 1999, 2003; Vlot et al., 2001; You et al., 2001; Zhang et al., 2004a) or in trans (Eckerle and Ball, 2002; Sit et al., 1998). Enhancers are generally found on viral minus-strands, need not be proximal to the core promoter, contain sequence and/or structural features of core promoters, and can promote transcription in the presence of sequences resembling the transcription initiation site (Nagy et al., 1999; Panavas and Nagy, 2003; Ray and White, 2003). Repressors (also known as transcriptional silencers) have recently been identified for members of the family *Tombusviridae* and are located on plus-strands just upstream from the core promoter. The positioning of transcriptional enhancing and repressing elements on opposite strands has led to the suggestion that these elements function to regulate asymmetric levels of plus- and minus-strand synthesis (Pogany et al., 2003).

Viruses in the family *Tombusviridae*, genus *Carmovirus*, are among the smallest (single RNA of 3.8–4.3 kb) and simplest (five to seven open reading frames) of the plus-strand RNA viruses (Simon, 2002). All carmovirus genomic RNAs (with the exception of *Galinsoga mosaic virus* [GaMV]) contain a 3′ proximal hairpin with a seven to 12 base pair stem just upstream of a C/GCCC-OH 3′ terminal sequence (Zhang et al., 2004a). Studies using a *Turnip crinkle virus* (TCV) satellite RNA (satC; 356 bases) that shares 88% sequence similarity with TCV in its 3′ 150 bases have demonstrated that this hairpin (Pr) comprises the core promoter for minus-strand synthesis (Song and Simon, 1995; Fig. 1A). With the exception of GaMV, all carmoviruses and satC also contain a second hairpin 15–27 bases upstream of Pr. These hairpins, designated as "H5," are topologically similar with a distinctive large internal symmetrical loop (LSL) that is A-rich on the 5′ side and G-rich on the 3′ side (Zhang et al., 2004a; Fig. 1B). H5 was recently determined to be a repressor of minus-strand synthesis in cell-free assays programmed with TCV RdRp purified from *Escherichia coli* (Zhang et al., 2004a). Repressor function required an interaction between the 3′ side of the LSL and the 3′ terminal GCCC-OH (Fig. 1A). An upstream 5′ sequence, termed a derepressor (DR), was necessary to relieve the repression by presumptively competing with H5 for interaction with 3′ terminal bases (Sun et al., 2004; Zhang et al., 2004a). Surprisingly, transcripts containing mutations in the TCV H5 LSL led to the generation of progeny in plants with as much as a 12-fold increase in second site mutations scattered throughout the sequenced region, with most alterations consisting of uridylate to cytidylate or adenylate to guanylate transitions (McCormack and Simon, 2004). This led to the proposal that H5 also functions as an RNA chaperone to aid in correctly assembling the RdRp complex. Members of the family *Tombusviridae* genus *Tombusvirus* also contain a similarly positioned hairpin (but with an internal asymmetrical loop) that is required in vivo (Fabian et al., 2003) and also functions as a repressor in cell-free assays by interacting with five 3′ terminal bases (Pogany et al., 2003).

Analysis of the LSL of satC H5 by in vivo functional selection (in vivo selex) revealed that nearly all positions in the middle and upper portions of the LSL were crucial for satC accumulation in protoplasts (Zhang et al., 2004b). For this report, we extend our analysis of H5 by examining sequence and structural preferences in the upper and lower stems using in vivo selex and exchanges with other carmoviral H5. Our results indicate that both sequence and structure are important in these H5 regions and confirm that H5 is a plus-strand element. We also demonstrate that enhanced fitness of some selex winners to accumulate in plants did not correlate with enhanced ability to replicate in protoplasts, suggesting that H5 might have additional, non-replication-related functions. Finally, we demonstrate that mutations in H5 strongly affect plus-strand as well as minus-strand accumulation, supporting a multifunctional role for this hairpin.

Results

The LSL and lower stem contribute significantly to H5 function in satC

The importance of H5 in minus-strand accumulation (Zhang et al., 2004a) and RdRp fidelity (McCormack and Simon, 2004) led to the initiation of a detailed characterization of satC H5 sequence and structure. Our initial characterization used site-specific mutagenesis and in vivo functional selex to examine the LSL (Zhang et al., 2004b). We determined that satC with various alterations in bases located in the lower two positions on either side of the LSL, including those that caused the bases to pair with their neighbors across the loop, could still accumulate to near wild-type (wt) levels or exceed wt levels in protoplasts. However, mutations in most other positions on both sides of the loop were extremely detrimental for satC accumulation. These results were not surprising given the strong conservation of the LSL, especially the upper region, among carmoviruses (Fig. 1B) and the interaction between the 3′ end and right side of the LSL that is necessary for proper initiation of satC in a cell-free assay programmed with RdRp purified from *E. coli* (Zhang et al., 2004a). The upper stem (US) and lower stem (LS) of H5 show much less sequence and structural conservation among carmoviruses (Fig. 1B). The US range from 3 to 7 base pairs and are

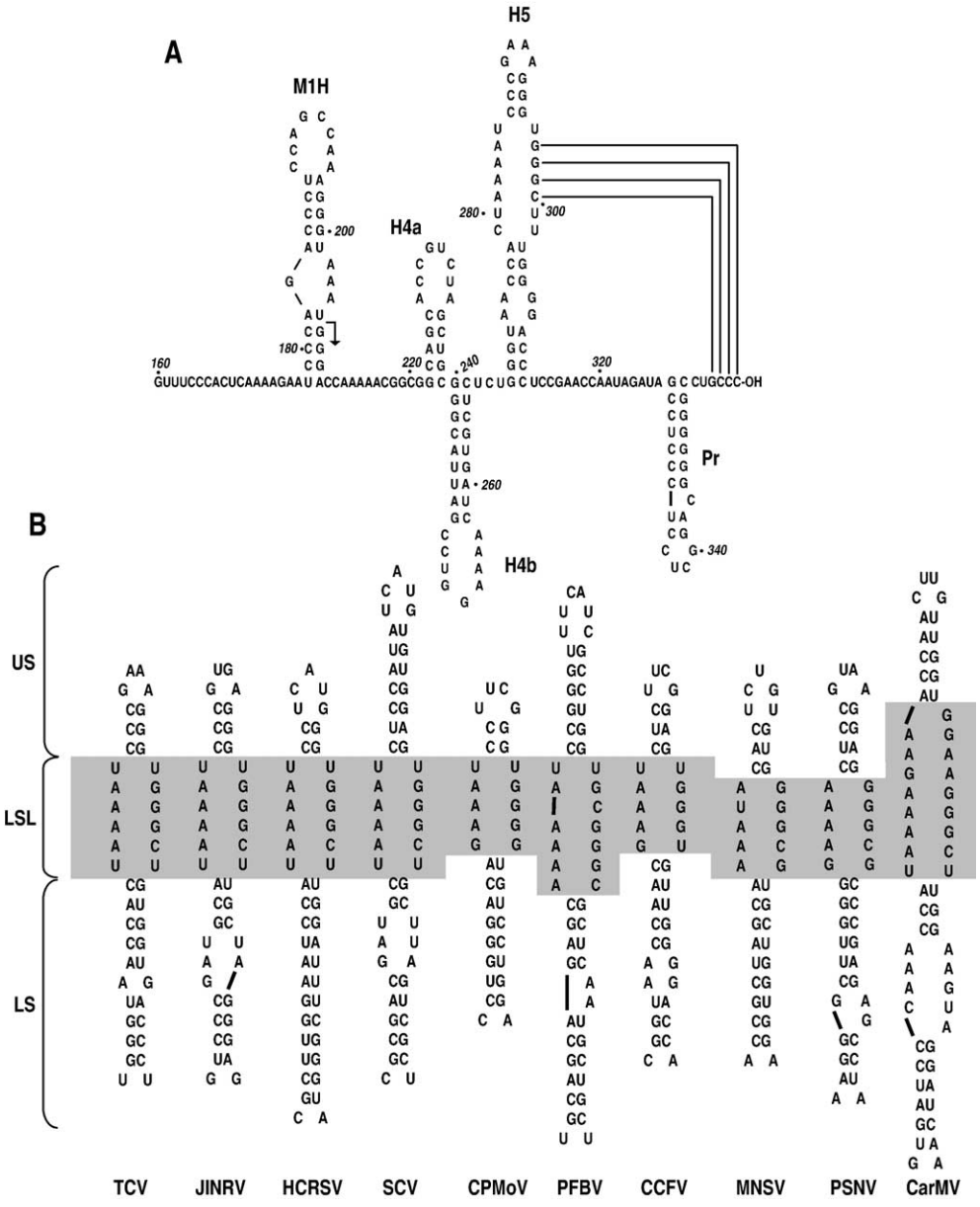

Fig. 1. Location and structure of Hairpin H5. (A) Structure of the 3′ region of satC. This structure was determined by a combination of chemical and enzymatic probing, computer modeling, and phylogenetic comparisons (Zhang et al., 2004a). Arrow denotes a contiguous 3′ end region shared between satC and TCV. Interaction between the 3′ terminal four bases and the H5 LSL is shown. Pr, core promoter. M1H, replication enhancer on minus-strands that also functions on plus-strands to repress TCV virion accumulation. H4a and H4b, hairpins that are structurally conserved among some carmoviruses. (B) H5 and single flanking bases present in TCV and other carmoviruses. The LSL region is shaded. JINRV, *Japanese iris necrosis virus*; HCRSV, *Hibiscus chlorotic virus*; SCV, *Saguaro cactus virus*; CPMoV, *Cowpea mottle virus*; PFBV, *Pelargonium flower break virus*; CCFV, *Cardamine chlorotic fleck virus*; MNSV, *Maize necrotic streak virus*; PSNV, *Pea stem necrosis virus*; CarMV, *Carnation mottle virus*.

capped by 4 to 6 base terminal loops in the 10 carmoviruses with available sequences. The LS range in length from 8 to 12 bases, and 7 of 10 carmoviral LSs are interrupted by a single internal symmetrical or asymmetrical loop of varying sequences.

To determine whether the US, LSL, and LS of satC are virus specific or whether these elements are exchangeable with their counterparts from other carmoviruses, the H5 of satC was precisely replaced with the H5 of *Japanese iris necrosis virus* (JINRV) and *Cardamine chlorotic fleck virus* (CCFV) (Fig. 2A). JINRV and CCFV H5 were selected for the following reasons. JINRV contains the identical LSL as TCV, which is identical to the LSL of satC at all but the lowest (and most flexible) position. The US of JINRV H5 is also nearly identical to that of satC, with the single base difference in the terminal loop still maintaining a highly stable GNRA tetraloop configuration (N is any nucleotide and R is a purine) (Moore, 1999). The LS of JINRV, however, differs at nearly every position from the LS of satC. In contrast, CCFV contains a truncated LSL compared

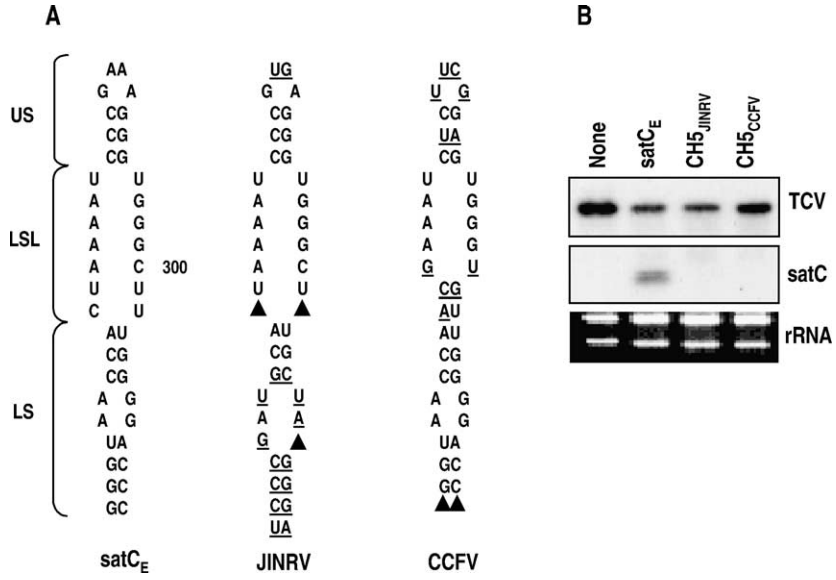

Fig. 2. Accumulation of satC containing heterologous carmovirus H5 in protoplasts. (A) Sequence differences among the satC, JINRV, and CCFV H5. Base differences are underlined. Triangles represent absent bases. SatC$_E$ is derived from satC by addition of two bases near the 3′ side of H5, which was required for ease in cloning. (B) Accumulation of satC$_E$ and satC$_E$ containing the H5 of JINRV (CH5$_{JINRV}$) or CCFV (CH5$_{CCFV}$). RNA was extracted from protoplasts at 40 hpi. The RNA gel blot was probed with an oligonucleotide specific for both satC and TCV. None, no satC in the inoculum. Ribosomal RNA (rRNA) levels were used as a loading control for all RNA gel blots in this study.

with satC with a notable cytidylate to uridylate difference at satC position 300. This positional variance maintains but weakens base-pairing with the 3′ end (see Fig. 1B), replacing a C•G pair with a U•G pair. The US of CCFV differs at six of nine positions with the US of satC including a C•G to U•A covariation in the stem and a highly stable UNCG tetraloop replacing the satC GNRA tetraloop. The LS, however, was nearly identical with that of satC, missing only a single base pair at the base and having two additional base pairs directly below the LSL.

Replacing satC H5 with H5 from CCFV and JINRV required the generation of a new *Eco*RV restriction site in the satC cDNA by insertion of two uridylates (after positions 316 and 317) near the 3′ base of the LSL. SatC with this alteration is denoted satC$_E$. SatC$_E$ containing either the H5 of JINRV (CH5$_{JINRV}$) or CCFV (CH5$_{CCFV}$) was assayed for accumulation at 40 h postinoculation (hpi) of *Arabidopsis thaliana* protoplasts. Plus-strands of both chimeric constructs did not accumulate to detectable levels when assayed by RNA gel blots, even following extensive overexposure of the blots (Fig. 2B). Since we had previously shown that the lowest position of the satC LSL (C279 and U302) could be base paired (as in TCV) without substantially altering satC levels in protoplasts (Zhang et al., 2004a), the inability of CH5$_{JINRV}$ to accumulate implied that the lower stem (the main difference between the JINRV and satC H5) must contribute significantly to the function of H5. The poor accumulation of CH5$_{CCFV}$ suggested that either the CCFV US or LSL was also incompatible with satC accumulation.

To better understand the relative contribution of the three H5 domains (US, LSL, and LS) to H5 function, satC$_E$ constructs were generated where one or two of the satC domains were converted to CCFV domains and the chimeric constructs assayed for accumulation in protoplasts (Fig. 3A). At 40 hpi, none of the chimeric H5 constructs accumulated to satC$_E$ levels (Fig. 3B). The CCFV US replacement construct (construct US) was the least debilitated, accumulating to 58% of satC$_E$ levels. Replacement of both the satC US and LSL with that of CCFV (construct US/LSL) or replacement of just the LSL (construct LSL) resulted in a 14- or 8-fold reduction in satC accumulation, respectively. It should be noted that the CCFV LSL domain transferred to satC in both of these constructs arbitrarily included the two base pairs directly below the LSL. These results suggest that weakening the base-pairing between the 3′ end and the CCFV LSL is detrimental to satC. However, additional factors, such as the inclusion of the two base pairs flanking the LSL, may also have contributed to reducing satC accumulation. Unexpectedly, there was a substantial effect of replacing the satC LS with that of CCFV (construct LS). Although construct LS differed from satC$_E$ by only a single G•C base pair at the base of the LS (present in satC [positions G270 and C311] and absent in CCFV), it accumulated to just 26% of satC$_E$ levels. This suggests that the length or stability of the lower stem is important for H5 function in satC. Replacement of both the LS and US with that of CCFV further reduced accumulation to only 10% of satC$_E$ levels. The most debilitating replacement was a combination of the CCFV LSL and LS, with the chimeric satC not accumulating to detectable levels. Altogether, these results suggest that efficient functioning of H5 in vivo requires all three H5 regions but is most dependent on the cognate LSL and LS.

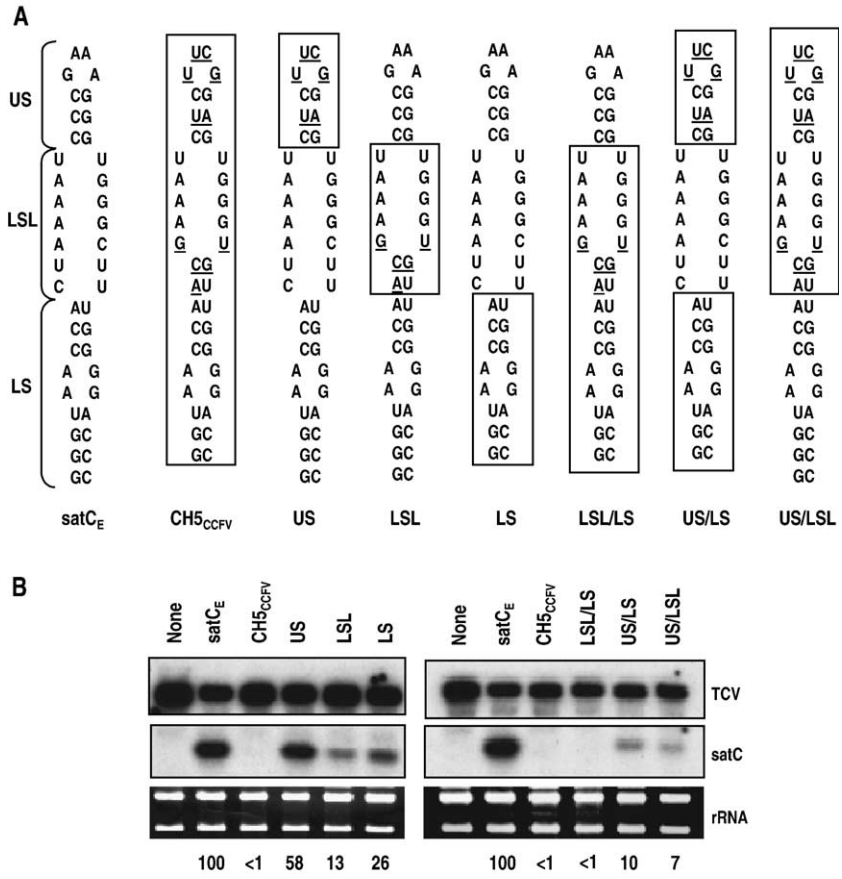

Fig. 3. Replacing the US, LS, and LSL of satC with that of CCFV. (A) Boxed sequences indicate portion of H5 that is derived from CCFV in the chimeric satC constructs. Base differences are underlined. Names of the constructs are given below the sequences. (B) RNA gel blot of viral RNAs accumulating in protoplasts at 40 hpi. The blots were probed with an oligonucleotide complementary to both satC and TCV. Values given below the blots are the averages of two independent experiments, with the satC$_E$ level arbitrarily assigned a value of 100. Names of the constructs are from (A). None, no satC in the inoculum.

In vivo selex of the satC US

To further characterize the sequence and structural requirements for the satC US and LS, both elements were independently subjected to in vivo functional selection (in vivo selex). In vivo functional selection is performed by randomizing all positions in a particular element, and then subjecting the randomized satC population and helper virus to selection for fitness through multiple rounds of competition in host plants. This selection strategy is possible because satC enhances the fitness of TCV by positively influencing virus movement through interference with virion formation (Zhang and Simon, 2003a); fewer assembled virions increase the amount of free coat protein available to suppress RNA silencing, an endogenous antiviral defense system (Qu et al., 2003; Thomas et al., 2003). TCV that is isolated from systemic leaves is therefore more likely to be associated with a functional satRNA. In vivo genetic selection is advantageous over site-specific mutagenesis in that selection is for fitness regardless of function and therefore can reveal additional functional roles of elements (Sun and Simon, 2003; Sun et al., 2004; Zhang and Simon, 2003b). In addition, since all positions in an element (or a portion of an element) are randomized, the necessity for a specific base is not judged in a remaining wt context.

SatC transcripts containing 10 randomized bases in place of the US were inoculated onto 30 plants and RNA was extracted from systemic leaves 3 weeks later. Ethidium bromide staining of agarose gels used to examine the RNA from these plants revealed that all plants examined accumulated wt levels of satC (data not shown; satC normally accumulates to levels similar to 5S ribosomal RNA). A total of 45 satC clones comprising 29 different US sequences were generated from 10 randomly selected plants and sequenced (first round selex winners; Fig. 4). Up to 5 different satC were isolated from any one plant and satC with identical US sequence were not isolated from multiple plants. Examination of the sequences revealed a preference for three base pair stems closed by a terminal four-base loop (20 of 29). The four-base loops varied in sequence with one comprising the wt GNRA tetraloop (U2) and four containing the very stable UNCG tetraloop (U5, U6, U18, and U19). Four of 29 clones had only a two base pair stem terminating in a six-base loop. Three clones contained sequence that would extend the stem of the US when the remainder of the H5 sequence is considered (boxed in Fig.

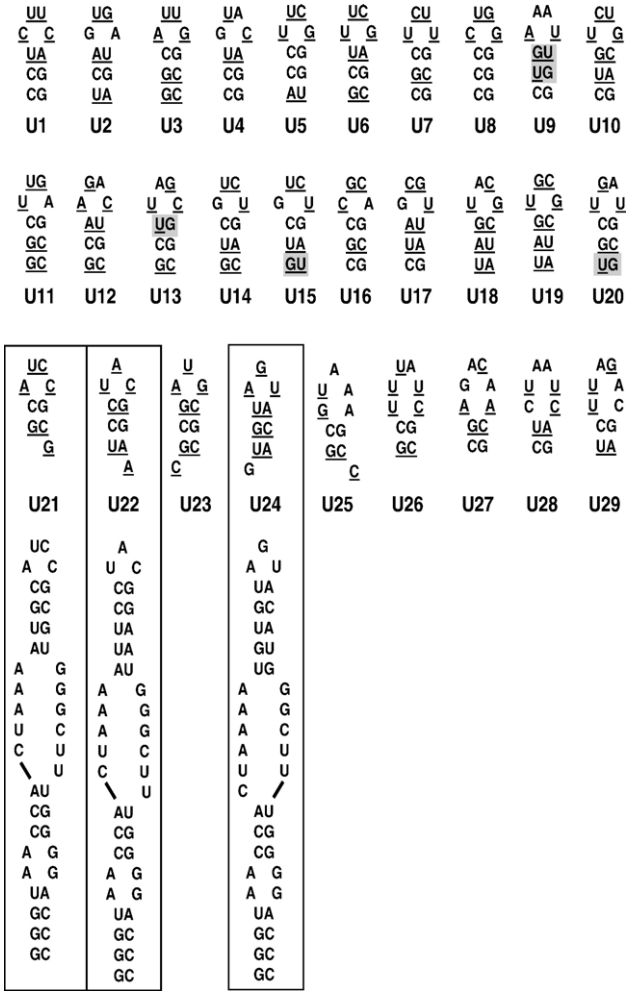

Fig. 4. First round US selex winners. SatC containing randomized bases replacing the US were inoculated with TCV onto 30 turnip plants. SatC species accumulating 3 weeks later were cloned and sequenced from 10 plants. No particular sequence was found in more than one plant. Differences with wt satC US sequences are underlined. Clones containing "orphaned" bases that can putatively base pair with an LSL base thus expanding the US (as indicated) are boxed. G•U base pairs (suggesting a plus-strand structure) are shaded. U21 had a single base deletion in the selexed region.

4) and five clones (U21 through U25) would presumably cause the LSL to no longer be symmetrical. Four of the clones contained G•U or U•G pairs, supporting the formation of H5 on plus-strands. While no fully wt sequences were recovered, the compositions of the stem sequences were not random. C•G was the preferred base pair (34 of 81 positions), followed by G•C (21 of 81), U•A (15 of 81), A•U (6 of 81), G•U, and U•G (5 of 81). Analysis of the US in natural carmoviral H5 revealed a similar preference for C•G (24 of 38) over G•C (2 of 38) (Fig. 1B).

To further explore the composition of US sequences that are beneficial to satC accumulation in plants, equal portions of RNA from the 30 first round plants were combined and used to inoculate six additional plants. After 3 weeks, RNA was extracted from systemic leaves of each plant and 37 clones were generated and sequenced (Fig. 5A). The sequences were not previously identified among the first round winners, indicating the likelihood that many more functional US sequences were present but not isolated from first round plants. Of the second round winners, only one clone was isolated from all six plants (U30), comprising 16 of the 37 clones sequenced. This clone contained a UNCG tetraloop and two of three C•G base pairs. All other clones were isolated from only one or two plants and contained four or six base terminal loops. As with the first round winners, the second round winners were most likely to have C•G (16 of 32 positions) or U•A (8 of 32) base pairs in the stem.

RNA from the six second round plants was pooled and used to inoculate six new plants, producing the final third round winners. Out of the 32 clones sequenced from these six plants at 3 weeks postinoculation, U30 again was the only clone found in all six plants (Fig. 5B). Two other clones from the second round were also recovered (U32 and U34) along with five new clones (U42 through U46). One of the new clones, U42, differed from second round winner U40 by a single uridylate to adenylate transversion that converted a two base pair stem/six base loop configuration to a three base pair stem/GNRA tetraloop. In our experience, in vivo selex frequently results in evolution of particular sequences to more fit sequences in later rounds due to the high frequency of RdRp errors, and thus it is likely that U42 was derived from U40. Sequence evolution was also apparent for some of the other third round winners: U45 differed from second round winner U37 by a single position in the four base terminal loop; U46 differed from U30 by a single change that maintained the UNCG tetraloop.

Because of sequence evolution, the number of recovered clones in the third and final round did not necessarily indicate which clones represent the most fit satRNA. To

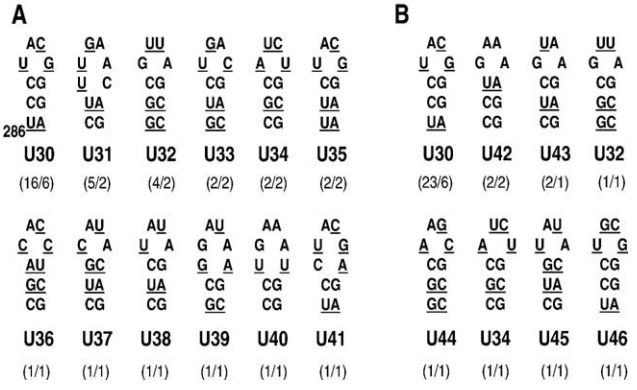

Fig. 5. Second and third round US selex winners. (A) Second round winners. (B) Third round winners. Equal amounts of RNA from first or second round plants were combined and used to inoculate six plants. SatC accumulating 3 weeks later were cloned and sequenced. The first number in the parentheses below each clone represents the total number of that clone in the sequenced population. The second number is the number of plants (out of six total) that contained the particular clone. Underlined bases differ from the wt satC US.

determine an approximate order of fitness of some selex winners, third round winners U30 (most prevalent) and U42 (most similar to wt satC; differed by only a single C•G to U•A covariation at position 288/293) along with second round winners U31 and U22 were subjected to direct competition. U31 and U22 were selected for inclusion in the competition assay because their US terminated in a six base loop or three base loop, respectively. In addition, U22 differed from U30 by only a single base difference yet contained a substantially altered structure (Fig. 6A). Three plants were inoculated with equal portions of transcripts derived from the four clones and progenies were examined from all plants at 3 weeks postinoculation. As shown in Table 1, third round winner U42 was the most fit among the clones assayed in plants, comprising 70% of the 26 sequenced clones. All remaining clones were U30. To determine the fitness of U42 and U30 compared with wt satC, additional competition assays were performed. U42 and wt satC were found to be of similar fitness, comprising

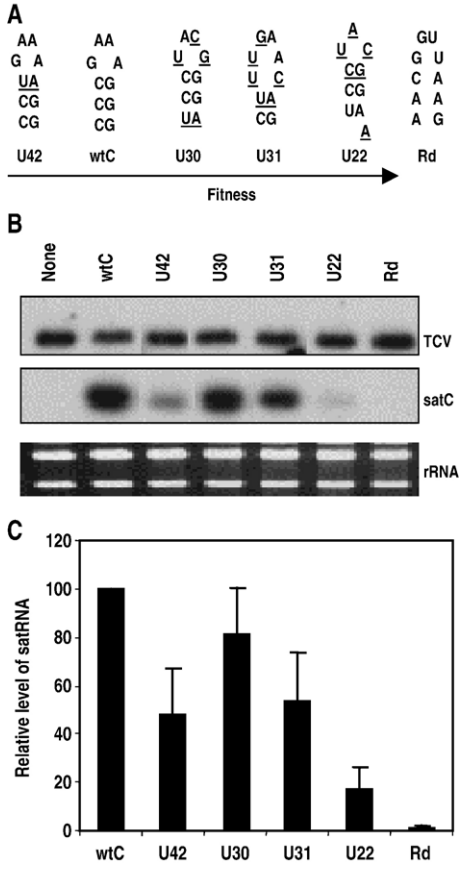

Fig. 6. Fitness of US selex winners to accumulate in protoplasts. (A) Fitness of clones to accumulate in plants (from Table 1). U42 and U30 were third round winners. U31 was a second round winner and U22 was a first round winner. Rd represents a randomly selected satC from the initial selex population generated by PCR. Underlined bases in the selex winners are positions that differ from wt satC (wtC). (B) Representative RNA gel blot of total RNA extracted at 40 hpi of protoplasts. None, no satC in the inoculum. (C) Quantification of satC accumulation levels. Data are from five independent repetitions.

Table 1
Competitions between third round selex winners and wt satC

	Clone	No. recovered from three plants
US		
Competition 1	U30	8
	U42	18
	U31	0
	U22	0
Competition 2	U42	17
	wtC	14
Competition 3	U30	9
	wtC	18
LS		
Competition 1	L3	0
	wtC	26

55% and 45% of the cloned population, respectively. Wt satC was more fit than U30, comprising 67% of the recovered clones. These results indicate a fitness order for accumulation in plants of U42 and wt satC, U30, followed by U31 and U22.

Fitness of satC to accumulate in plants reflects replication competence, stability, trafficking ability, and capacity of enhancing TCV movement. To determine if the satRNAs most fit to accumulate in plants were also the best templates for accumulation in protoplasts (which reflects only replication competence and stability), U42, U30, U31, and U22 were individually inoculated with helper virus onto protoplasts along with wt satC and satC containing a randomly selected UL sequence (Rd; Fig. 6A). Although U42 and wt satC were equally fit in plants, U42 accumulated to only 46% of wt satC levels and reached only 60% of U30 levels. The efficient accumulation of U30 (82% of wt satC) suggests that the highly stable satC GNRA tetraloop can be replaced by the equally stable UNCG tetraloop (Fig. 5B; Fig. 6C). This argues that the satC GNRA tetraloop is likely present to stabilize the H5 structure and is not involved in tertiary interactions with docking sequences (Abramovitz and Pyle, 1997).

In vivo selex of the satC LS

To investigate sequence requirements in the satC LS, 18 residues were randomized and the satC population was subjected to in vivo selex (Fig. 7A). Of the 60 plants inoculated with the satC population, only five contained satC detectable by agarose gel electrophoresis and ethidium bromide staining. Forty-six clones were isolated from these plants and the 10 unique sequences are presented in Fig. 7B. Clones isolated from the same plant had very similar sequence and likely originated from a single transcript followed by sequence evolution. Interesting features of the first round winners included the following: six to nine base pair stems in the selexed region; a weak base pair (U•A, U•G or A•U) at positions 278/303 just below the LSL in most sequences (A•U in wt satC); the lack of interruption of the base-paired region in most clones by symmetrical or asymmetrical interior loops; and a G•C pair in the first

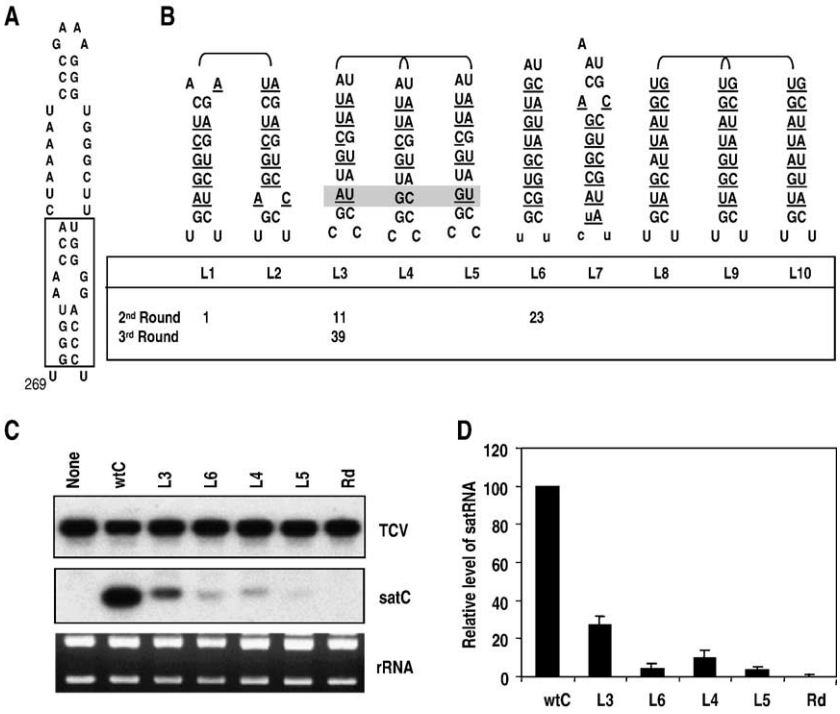

Fig. 7. Selex of the H5 LS. (A) SatC H5. Bases subjected to selex analysis are boxed. (B) LS selex winners. Sequences of clones found in first round plants are shown. Lines connecting sequences indicate isolation from the same plant. Bases that differ from wt satC LS are underlined. Names of the winners are shown below the sequences. Numbers of particular clones contained in the sequenced population from second and third round plants are given below the sequence names. Shading indicates the single positional differences among L3, L4, and L5. Lower case letters denote that these bases were not subjected to selection. (C) Representative RNA gel blot of total RNA extracted at 40 hpi of protoplasts. None, no satC in the inoculum. wtC, wt satC. Rd, satC with a randomly selected US sequence (5′ CACACUUAA-AUUCAACUC 3′). (D) Quantification of satC accumulation levels. Data are from three independent repetitions.

position of all stems with one exception. An additional common feature was the surprising presence of putatively single-stranded pyrimidines flanking the H5, which were identical pyrimidines in all of the sequences except L7 (satC and TCV H5 are flanked by uridylates). For L7, the base of the LS stem contained a single unpaired 3′ side adenylate in the selexed region that could pair with the 5′ uridylate flanking the selexed bases. This would place two non-identical pyrimidines flanking the H5. The presence of flanking pyrimidines was surprising given that they would be adjacent to the natural satC uridylates at positions 269 and 312. The presence of identical pyrimidines flanking H5 did not extend to most other carmoviral H5 (Fig. 1B), and thus the significance of this finding is not known.

For the second round, equal portions of RNA isolated from the 60 plants were pooled and used to inoculate six additional plants. Of the 35 clones generated following RNA extraction at 3 weeks postinoculation, only three sequences from the first round were represented and only two of these sequences were found in multiple plants (L3 and L6). L6 was the most prevalent second round winner, comprising 23 of the 35 clones. RNA from the six second round plants was pooled and used to inoculate six additional plants. In the third and final round, only L3 was found out of 39 clones sequenced. L3 differed from first round sister clones L4 and L5 at only a single position, the second base pair from the base of the stem (L3, A•U; L4, G•C; and L5, G•U). The enhanced fitness of L3 compared with L4 and L5 suggests that the identity of base pairs in the stem is important and not the absolute strength of the pairings.

L3 was subjected to direct competition in plants along with wt satC. All 26 clones isolated 3 weeks postinoculation were wt satC, indicating a strong preference for the wt LS stem. To determine if fitness to accumulate in plants correlated with enhanced accumulation in protoplasts, wt satC along with second round winners L3 and L6, and L3 sister clones L4 and L5 were examined for accumulation in protoplasts along with TCV helper virus. Third round winner L3 accumulated sevenfold better than second round winner L6 and three- to ninefold better than sister clones L4 and L5 (Table 1). However, L3 only accumulated to 27% of wt satC levels (Figs. 7C and D). The results of the LS selex support the need for a base-paired stem with sequence-specific preferences. However, poor accumulation of third round winner L3 compared to wt satC indicates that there was insufficient complexity in the initial population of randomized satC that entered plant cells with TCV to efficiently meet these two criteria.

Relationship between H5 and the previously characterized minus-strand element, 5′PE

We previously identified two short linear sequences as being redundant elements required for plus-strand synthesis

using minus-strand satC templates in our in vitro transcription system programmed with partially purified TCV RdRp (Guan et al., 1997). SatC containing mutations in one element, the 5′PE, replicated poorly in protoplasts, with a greater reduction in accumulation of plus-strands than minus-strands (Guan et al., 2000). Taken together, these results led to the suggestion that the 5′PE was a minus-strand element that functioned in plus-strand synthesis. However, 10 of 13 bases of the 5′PE comprise the complement of the 3′ side lower stem of H5 (positions 302–314; Fig. 8A). The importance of both sequence and structure of the lower stem of H5 for satC accumulation revealed in the current study required a re-investigation of the 5′PE to determine if it was truly an independent minus-strand element or whether the sequence functioned as a portion of the H5 LS. This latter explanation would indicate that H5 functions in both minus-strand and plus-strand accumulation.

We previously demonstrated that altering G304 to U (G304U) or A (G304A) was highly detrimental to satC accumulation in protoplasts, reducing plus-strands to below the level of detection while maintaining low levels of minus-strands (Guan et al., 2000). G304 is located in the middle position of the three base stem portion in the H5 LS, and thus these mutations are predicted to substantially alter the structure of H5 (Fig. 8A). Confirming previous results, satC plus-strands containing G304A or G304U did not accumulate to detectable levels, whereas minus-strands accumulated to 2% and 5% of wt satC levels, respectively (Fig. 8B). SatC with a new alteration at position 304, G304C, did not accumulate detectable levels of either plus- or minus-strands. Alteration of C277, which is proposed to pair with G304 in H5, to a guanylate (C277G) was also detrimental, with plus-strands accumulating to 1.5% of wt satC and minus-strands accumulating to 9% of wt satC. Combining G304C with C277G, which re-establishes base-pairing at this position in the hairpin, enhanced plus-strand accumulation to 17% of wt satC. These combined mutations had an even greater effect on minus-strand accumulation, enhancing the level of minus-strands to 56% of wt satC. When C277G was combined with G304U, which would allow for a G:U pairing at this position in plus-strands, satC plus-strands reached 26% of wt levels and minus-strand levels were enhanced to 67% of wt. Since G304A was highly detrimental despite allowing for a G:U pairing in a presumptive minus-strand H5 structure, these results support H5 as a plus-strand structure. In addition, these results suggest that the 5′PE is not an independent minus-strand element but that prior mutations in the 5′PE were detrimental because they affected the H5 LS.

All mutations tested resulted either in undetectable levels of plus- and minus-strands or in a disproportionate reduction of plus-strands. One possible explanation for this effect is if the H5 LS mutations reduce the stability of plus-strands. To test for this possibility, protoplasts were inoculated with wt satC or satC containing C277G/G304C, C277G/G304U, or G304C in the absence of TCV and undegraded RNA examined between 1 and 6 h postinoculation by Northern blots. No significant differences in the rate of RNA degradation were found between wt satC and any of the mutants (data not shown). This result suggests that H5 has a functional role in the accumulation of both strands.

To support the conclusion that the 5′PE is not an independent minus-strand element, H5 of satC was precisely

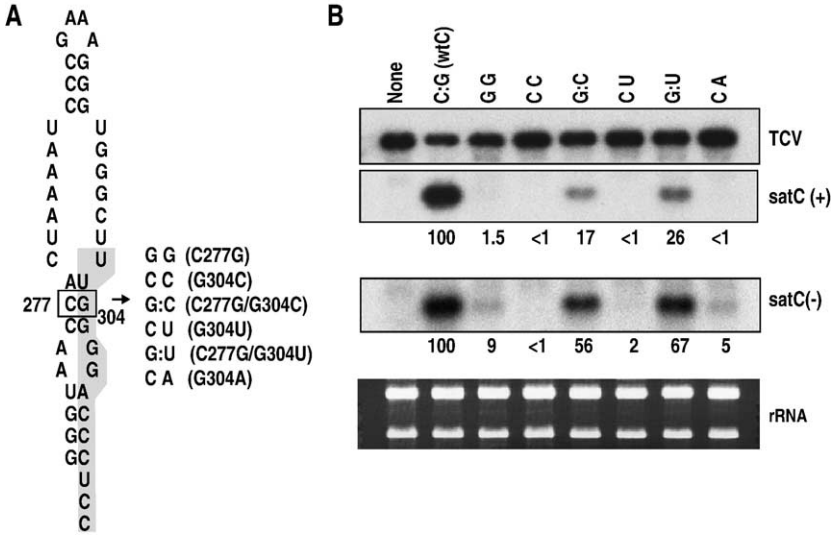

Fig. 8. Mutational analysis of the upper portion of the H5 lower stem. (A) Single or double mutations were constructed at positions 277 and/or 304 in satC leading to the plus-strand pairings at this position as shown. Names of the mutants are given to the right in parentheses. The sequence complementary to the previously described 5′PE is shaded. (B) SatC containing these mutations were inoculated onto protoplasts along with TCV helper virus and satC accumulating at 40 hpi was examined by RNA gel blots using plus- or minus-strand specific probes. Letters above each lane denote the identity of the residues in position 277 and 304. Numbers below the panels are the average values from two independent experiments. None, no satC in the inoculum; wtC, wt satC.

replaced with H5 of TCV, generating $CH5_{TCV}$ (Fig. 9A). TCV H5 differs from satC H5 at positions 302 and 306 within the complementary 5′PE sequence, which results in a five base-stem just below the H5 LSL compared with a three-base stem for satC H5. The analogous position to G304 in TCV H5 is located in the center of the five-base stem, and thus altering this position should not be as disruptive to the structure of TCV H5. $CH5_{TCV}$ consistently accumulated to slightly higher levels than wt satC in protoplasts indicating that the two base differences between the satC and TCV H5 do not negatively impact on the replication of satC (Fig. 9B). Plus-strands of $CH5_{TCV}$ containing G304A or G304U accumulated to 58% and 59% of wt satC levels, respectively, compared with undetectable levels for the analogous satC mutants. The same mutations generated in wt TCV H5 (G3971C, G3971U, or G3971A) also had only a marginal effect on TCV accumulation, with levels reaching 90%, 90%, or 79% of wt TCV levels, respectively (Fig. 9C). Altogether, these results indicate that mutations that disrupt satC H5 impair plus- and minus-strand accumulation and that the complementary sequence to the H5 3′ side lower stem may not have an independent role in satC replication.

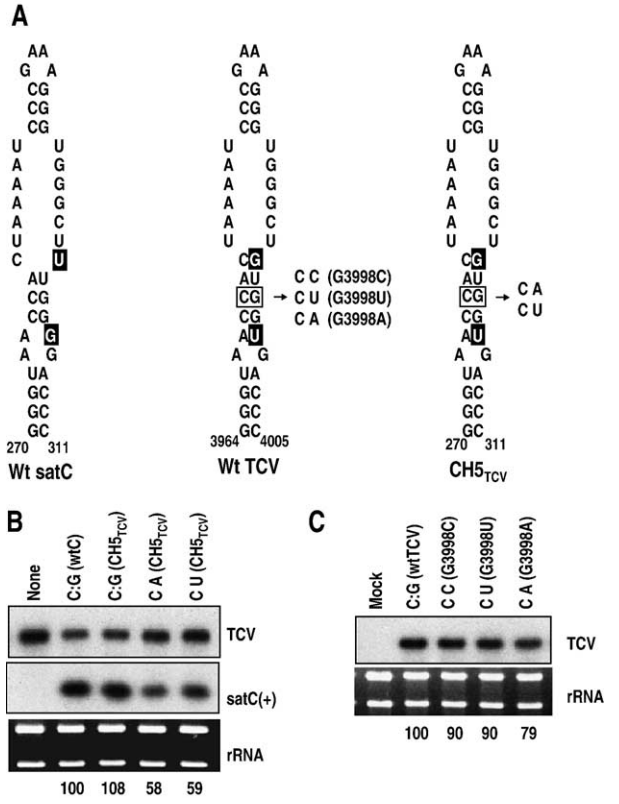

Fig. 9. Effect of mutations at position 304 on the analogous location in TCV H5 and in satC containing H5 of TCV. (A) Single mutations were generated in TCV H5 or in satC with H5 of TCV ($CH5_{TCV}$) as shown. Names of the TCV mutants are given in parentheses. Residues boxed in black denote differences between H5 of satC and TCV. (B) $CH5_{TCV}$ containing the alterations shown in A were inoculated onto protoplasts along with TCV helper virus and satC accumulation accessed at 40 hpi. Letters above each lane denote the identity of the residues in position 277 and 304. Only satC plus-strands are shown. Numbers below the panels are the average values from two independent experiments. None, no added satRNA; wtC, wt satC. (C) TCV containing the mutations shown in A was inoculated onto protoplasts and the level of viral RNA accumulating at 40 hpi was examined by RNA gel blots. Letters above each lane denote the identity of the residues in positions 3971 and 3998. Numbers below the panel are the average values from two independent experiments. Mock, no TCV in the inoculum.

Discussion

Prior reports indicated an important role for H5 in satC and TCV replication in vivo (McCormack and Simon, 2004; Zhang et al., 2004a, 2004b) and in transcription in vitro using purified TCV RdRp (Zhang et al., 2004a). It was suggested that H5 is involved in the correct assembly of the RdRp since mutations in the TCV H5 LSL caused a significant increase in mutation frequency (McCormack and Simon, 2004). While carmoviral H5 have varying degrees of sequence similarity, all are topologically similar and capable of forming four base pairs between their 3′ side LSL and the 3′ terminus of the genomic RNA, suggesting that this interaction is also necessary for proper viral replication (Zhang et al., 2004a). Tombusvirus hairpin SL3, which also interacts with 3′ terminal sequences, likely performs a function analogous to the *Carmovirus* H5 (Fabian et al., 2003; Pogany et al., 2003).

The current report indicates, however, that H5 are not functionally interchangeable even when base-pairing between the LSL and 3′ end is putatively maintained. Despite similarity between the JINRV and satC LSL, differing only in the lowest and most flexible position, satC with H5 of JINRV did not accumulate to detectable levels in protoplasts. This suggests that the US or LS of JINRV is not compatible with the remaining satC sequence. Selex of the satC US indicates a preference for a stable tetraloop closed by a C•G base pair with at least one additional C•G pair in the short stem. However, a variety of other sequence/structural combinations were also functional, indicating substantial plasticity in the upper portion of the hairpin. This suggests that the two positional differences between satC and JINRV H5 tetraloops, which maintain the GNRA configuration, are not likely responsible for the negative effect on satC accumulation and suggest instead that the JINRV LS is incompatible with satC accumulation.

Exchanging the satC US, LSL, and/or LS with equivalent regions from the CCFV H5 supports the importance of the cognate LS for H5 function. The absence of a single G:C pair at the base of the LS (construct LS, Fig. 3) resulted in a 74% decrease in satC accumulation in protoplasts. The most debilitating exchange of individual H5 regions was the replacement of the satC LSL with the CCFV LSL (construct LSL, Fig. 3), which reduced accumulation by 87%. However, this construct also extended the LS by two base pairs, and thus it is not known whether the elongation of the

LS or the base differences in the LSL are responsible for the negative effect on satC replication. In vivo selex of the satC H5 LS confirmed the importance of both structure and sequence of the LS. With only one exception, all winners contained a G:C pair at the base of the LS flanked by unpaired, identical pyrimidines and a weak base pair adjacent to the LSL. In addition, the single covariant position in the LS winners L3, L4, and L5 had a substantial effect on satC accumulation in protoplasts that was unrelated to the strength of the paired bases. The importance of both structure and sequence of the LS is also supported by results that indicated enhanced satC accumulation with a G•U replacing the C•G at positions 277/304 compared with a G•C (Fig. 8).

Altogether, these results suggest that the H5 LS functions in more than a purely structural role supporting the phylogenetically conserved structure of H5. While it is possible that factors interacting with H5 may require LS functional groups in specific locations, it is also possible that H5 undergoes a structural rearrangement as part of its role in satC replication. Deletion of the 3′ terminal three cytidylates significantly alters the structure of H5 and 3′ flanking sequences without substantially affecting the remainder of satC (Zhang et al., 2004a). Such structural rearrangement of H5 might involve a secondary interaction between LS sequences and other partner sequences, thus constricting the nature of bases in the stem. Several recent findings support a role for sequences external to H5 in supporting H5 function. Wang and Wong (2004) determined that the poor ability of TCV H5 to substitute for the H5 of HCRSV could be improved by co-transferring the TCV Pr core promoter hairpin. In addition, mutations in the LS of TCV H5 that affected the small interior loop led to second site alterations in the nearby hairpin H4b (R. Zamora and A.E. Simon, unpublished results). All together, these results suggest that complex interactions between H5 and other sequences in satC are likely required for efficient replication.

The importance of the H5 LS for H5 function also explains previous results on an element we named the 5′PE. This element was first identified as required for transcription of plus-strands from minus-strand templates in vitro in the absence of 3′ proximal sequences (Guan et al., 1997). The element was able to independently promote complementary strand synthesis in vitro, and mutations in the sequence within satC resulted in an enhanced reduction of plus-strands compared with minus-strands in vivo. Taken together, these results supported the hypothesis that the 5′PE was a minus-strand element involved in plus-strand accumulation. However, the mutations constructed in the 5′PE are now predicted to substantially alter the structure of H5 on the complementary plus-strand. Analogous mutations in satC with H5 of TCV ($CH5_{TCV}$), which disrupt the center of a five base stem in the LS (compared with disrupting the center of a three base stem for satC H5), had a much reduced effect on accumulation of satC (Fig. 9B). This suggests that the previous mutations in satC were partially or fully disrupting H5 function rather than the complementary sequence. The sequence-specific nature of the winners of our previous in vivo selex of the 5′PE (Guan et al., 2000; shaded sequence in Fig. 8A) can now be explained by a requirement to maintain the sequence and structure of the LS. Interestingly, this selex revealed that the UCC flanking the 3′ side of H5 was conserved in all winners and could be preceded by a random base. We are currently addressing the role of the linker sequence between H5 and Pr in satC and TCV replication.

All mutations tested at positions 277 and 304 in the satC LS caused a greater reduction in the accumulation of plus-strands compared with minus-strands. This suggests that H5 may function in plus-strand as well as minus-strand accumulation. Elements located proximal to the 3′ end of plus-strands that disproportionately reduce the accumulation of plus-strands compared with minus-strands have also been found for other viruses. For example, deletion of the 3′ UTR of poliovirus resulted in the reduction of plus-strands to only 10% of wt levels in neuronal cells without decreasing minus-strand levels (Brown et al., 2004). In *Potato virus X* (PVX), mutations that affected either a 3′ proximal plus-strand hairpin or a putative polyadenylation signal reduced progeny plus-strands by 65–80% compared with minus-strand reductions of only 30–40% (Pillai-Nair et al., 2003). In both examples, instability of mutated plus-strands was not responsible for the reduction in plus-strand levels (Brown et al., 2004; Hemenway, personal communication). Instability of mutant plus-strands was also not a factor for several satC H5 mutants tested (data not shown). A second possibility for how a plus-strand element can affect plus-strand synthesis is if the element alters the structure of the RdRp or assembly of the replicase complex, which may have distinct forms for transcription of minus and plus-strands. Synthesis of plus- and minus-strands by two replication complexes with differing stabilities has been shown for Sindbis virus (Dé et al., 1996). Our previous suggestion that H5 may be nucleating the TCV replication complex (McCormack and Simon, 2004) supports this possibility.

The results of the in vivo selex of the US indicate that enhanced fitness of winner U42 in plants did not correlate with enhanced accumulation in plant cells. This supports findings from the previous satC LSL selex that fitness in plants of H5 mutants does not always correlate with increased accumulation in protoplasts (Zhang et al., 2004b). Currently it is not known what additional role(s) outside of replication might require H5. Past in vivo selex of the satC minus-strand M1H enhancer revealed that one of the most fit winners replicated only marginally better than random sequence. This winner, however, was shown to be exceptionally efficient at reducing virion formation (due to a hairpin that formed on the plus-strand), thus enhancing the ability of TCV to overcome RNA silencing (Zhang and Simon, 2003b). Whether H5 is also involved in reducing virion levels has not yet been explored.

Materials and methods

Construction of satC mutants

For generation of satC with H5 (or H5 portions) of CCFV or JINRV, an *Eco*RV restriction site was generated downstream of H5 in pT7C(+), which contains full-length cDNA of satC downstream of a T7 RNA polymerase promoter (Song and Simon, 1994). CEcV and T7C5′ were used as primers (a list of primers used in this study is presented in Table 2) in a PCR, and products were cloned into the *Sma*I site of pUC19 generating pT7CEcV. $CH5_{JINRV}$ and $CH5_{CCFV}$ were constructed by PCR using pT7C(+) as template and T7C5′ and JINRVH or CCFVH as primer, respectively. Following digestion with *Eco*RV and *Nco*I, the fragment was inserted into the analogous location in pT7CEcV, which had been treated with the same restriction enzymes. LSL/LS and US/LS were generated in a similar fashion except that $CH5_{CCFV}$ was used as template and CCFV-UC and CCFV-IC were used with T7C5′ as primers, respectively. For construction of US/LSL and LSL, oligonucleotide CCFV-LC5 and CCFV-LC3 were used for PCR. The templates were constructs $CH5_{CCFV}$ and LSL/LS, respectively. PCR products were subsequently digested with *Spe*I and *Eco*RV and cloned into pT7CEcV replacing the analogous wt fragment. To generate US, PCR was performed with primers C-5Uf and CEcV and construct US/LS. PCR products were digested with *Spe*I and *Eco*RV and cloned into pT7CEcV that had been treated with the same restriction enzymes. LS was generated in a similar fashion, except C-5Lf and C-3Lf were used as primers and pT7C(+) was used as template. For construction of $CH5_{TCV}$, oligonucleotides T7C5′ and T5PC were used as primers with template pT7C(+). PCR products were treated with *Spe*I and T4 polynucleotide kinase and inserted into the analogous location in pT7C(+) that had been treated with *Spe*I and *Sma*I. G304C and C277G were generated in a similar fashion except that oligonucleotides T7C5′ and G304C or G277C and oligo 7 were used as primers, respectively. C277G/G304U was generated in a similar fashion except that pT7M3 (Guan et al., 2000) was used as template. C277G/G304C was also generated similarly with oligonucleotides C277G and G304C as primers. $CH5_{TCV}$G304A and $CH5_{TCV}$G304U were generated by PCR using oligonucleotides T7C5′ and T5PCm with pT7C(+) as template. PCR products were cloned into the *Sma*I of pUC19. Mutants were identified by sequencing.

Construction of TCV mutants

G3998C, G3998U, and G3998A were generated by PCR using plasmid pTCV66 as template. pTCV66 contains wt TCV cDNA downstream from a T7 RNA polymerase promoter. Oligonucleotides SEQ1 and KK57 were used as primers. Following treatment with T4 polynucleotide kinase and *Spe*I, the fragment was cloned into the analogous location in pTCV66, which had been treated with *Spe*I and *Sma*I. Mutants were identified by sequencing.

In vitro transcription, inoculation of Arabidopsis protoplasts, and RNA gel blots

TCV genomic RNA was synthesized using T7 RNA polymerase and plasmids previously digested with *Sma*I, which generates transcripts with precise 5′ and 3′ ends. SatC transcripts were synthesized from plasmids linearized with *Sma*I (for chimeric H5 constructs) or directly from PCR products (for selex winners, using primers T7C5′ and oligo 7). Protoplasts (5×10^6), prepared from callus cultures of *Arabidopsis thaliana* ecotype Col-0, were inoculated with 20 μg of TCV genomic RNA transcripts with or without 2 μg of satC RNA transcripts using PEG-$CaCl_2$, as previously described (Kong et al., 1997). Total RNAs were isolated from protoplasts at 40 hpi and subjected to RNA gel blot analysis. Plus-strand RNA was probed with [γ-^{32}P]ATP-labeled oligo 13, which is complementary to both satC and TCV sequence (Zhang and Simon, 2003b). For analysis of minus-strands, RNA was probed with a [α-^{32}P]UTP-labeled riboprobe obtained from *Dra*I-digested pT7C(+) following transcription with T7 RNA polymerase (Nagy et al., 1999).

In vivo selex

In vivo selex was performed as previously described (Zhang et al., 2004b). Full-length satC cDNAs containing randomized bases in the H5 LS and US were generated by PCR using pNco-C277 (Zhang et al., 2004b) as template. Primers used were T7C5′ and either 3CTS or CLoS, respectively. PCR products were purified and directly subjected to in vitro transcription using T7 RNA polymerase. The number of cDNA molecules used for in vitro transcription of RNA to infect one plant was 4×10^{12}.

For the first round selex, 5 μg of satC transcripts containing randomized LS or US sequences was inoculated onto each of 60 (LS selex) or 30 (US selex) turnip seedlings along with 4 μg of TCV transcripts. Total RNA was extracted from uninoculated leaves at 21 dpi. Viable satC species were recovered by RT-PCR using oligonucleotides C5′ and oligo 7, cloned into the *Sma*I site of pUC19 or pGEM-T and sequenced. For the second round, equal amounts of leaf tissue from each plant were combined, and total RNA was extracted and then inoculated (~5 μg/plant) onto six turnip seedlings. For the third round, equal amounts of total RNA, extracted from each plant of the previous round, were pooled and then inoculated onto six turnip seedlings (~5 μg/plant). SatC species at 3 weeks postinoculation were cloned and full-length sequences were sequenced.

Table 2
Summary of the oligonucleotides used in this study

Application/ construct	Name	Position[a]	Sequence[b]	Polarity[c]
Mutagenesis in satC H5	T7C5′	1–19	5′-*GTAATACGACTCACTATA*GGGAUAACUAAGGGTTTCA	+
	C5′	1–19	5′-GGGAUAACUAAGGGTTTCA	+
	CEcV	300–356	5′-GGGCAGGCCCCCCGTCCGAGGAGGGAGGCTATCTATTG (G**A**T**A**TC) GGAGGGTCCCCAAAG	–
	JINRVH	252–322	5′-ATTG (G**A**T**A**TC) GGATCCCTAGCAAGCCCACCCTCACGGGATTTTATGCATCGGGAAGAGAGCACTAGTTTTCC	–
	CCFVH	252–322	5′-ATTG (G**A**T**A**TC) GGAGGTCCCCAACACCCACTCCGAAGAGATTTCGTTGGTTACCAGAGAGCACTAGTTTTCC	–
	CCFV-UC	271–322	5′-ATTG (G**A**T**A**TC) GGAGGTCCCCAACACCCACCCTTTCGGGATTTCGTTGGTTACC	–
	CCFV-IC	264–322	5′-ATTG (G**A**T**A**TC) GGAGGTCCCCAAAGCCCACTCCGAAGAGATTTTAGTGGTTACCAGAGAG	–
	CCFV-LC5	257–281	5′-aACTAGTGCTCTCTGGGTAACCAACG	+
	CCFV-LC3	298–322	5′-ATTG (G**A**T**A**TC) GGAGGGTCCCCAACACC	–
	C-5Lf	257–279	5′-gACTAGTGCTCTCTGGTAACCAC	+
	C-3Lf	299–322	5′-ATTG (G**A**T**A**TC) GGAGGTCCCCAAAGC	–
	C-5Uf	257–279	5′-gACTAGTGCTCTCTGGGTAACCAC	+
	T5PC	289–356	5′-GGGCAGGCCCCCCGTCCGAGGAGGGAGGCTATCTATTGGTTCGGAGGGTCACCACAGCCCACCCTTTC	–
	T5PCm	289–356	5′-GGGCAGGCCCCCCGTCCGAGGAGGGAGGCTATCTATTGGTTCGGAGGGTCACNACAGCCCACCCTTTC	–
	C277G	257–289	5′-gcacACTAGTGCTCTCTGGGTAACGACTAAAATCCCG	+
	G304C	288–356	5′-GGGCAGGCCCCCCGTCCGAGGAGGGAGGCTATCTATTGGTTCGGAGGGTCCCGAAAGCCCACCCTTTCG	–
	oligo 7	338–356	5′-GGGCAGGCCCCCCGTCCGA	–
Mutagenesis in TCV H5	SEQ1	3947–4009	5′-GAAAACTAGTGCTCTTTGGGTAACCACTAAAATCCCGAAAGGGTGGGCTGTHGTGACCCTCCG	+
	KK57	4036–4054	5′-GGGCAGGCCCCCCCCCCGC	–
Selex	3CTS	266–356	5′-GGGCAGGCCCCCCGTCCGAGGAGGGAGGCTATCTATTGGTTCGGAGGGTCCCCAAAGCCCANNNNNNNNNNATTTTAGTGGTTACCCAGAG	–
	CLoS	252–356	5′-GGGCAGGCCCCCCGTCCGAGGAGGGAGGCTATCTATTGGTTCGGANNNNNNNNNNAAGCCCACCCTTTCGGGATTTTAGNNNNNNNNNNAGAGAGCACTAGTTTTCC	–
RNA gel blots	oligo 13	249–269	5′-AGAGAGCACTAGTTTTCCAGG[d]	–

[a] Coordinates correspond to those of the TCV genome (SEQ1 and KK57) or satC (all the other oligonucleotides).
[b] Bases in italics indicate T7 RNA polymerase promoter sequence. Bold residues denote bases inserted to generate an *Eco*RV site (in parentheses). Bases in lowercase were added to achieve efficient digestion. "N" represents randomized bases. "H" represents mixed base A, C, and T. Mutant bases are underlined.
[c] "+" and "–" polarities refer to homology and complementarity with sat C plus-strands, respectively.
[d] Oligo 13 is also complementary to positions 3950–3970 of TCV genomic RNA.

In planta competition of selex winners

Equal amounts of transcripts were combined and used to inoculate three turnip seedlings (0.4 μg/plant) along with TCV genomic RNA transcripts (4 μg/plant). SatC species from all plants at 3 weeks postinoculation were cloned and assayed as described above.

Acknowledgments

We are grateful to Mr. Robert M. Stuntz for technical support. Funding was provided by grants from the U.S. Public Health Service (GM61515-01) and the National Science Foundation (MCB-0086952) to AES.

References

Abramovitz, D.L., Pyle, A.M., 1997. Remarkable morphological variability of a common RNA folding motif: the GNRA tetraloop-receptor interaction. J. Mol. Biol. 266, 493–506.

Barton, D.J., O'Donnell, B.J., Flanegan, J.B., 2001. 5′ cloveleaf in poliovirus RNA is a *cis*-acting replication element required for negative-strand synthesis. EMBO J. 20, 1439–1448.

Brown, D.M., Kauder, S.E., Cornell, C.T., Jang, G.M., Racaniello, V.R., Semler, B., 2004. Cell-dependent role for the poliovirus 3′ noncoding region in positive-strand RNA synthesis. J. Virol. 78, 1344–1351.

Buck, K.W., 1996. Comparison of the replication of positive-stranded RNA viruses of plants and animals. Adv. Virus Res. 47, 159–251.

Chapman, R.M., Kao, C.C., 1999. A minimal RNA promoter for minus-strand RNA synthesis by the brome mosaic virus polymerase complex. J. Mol. Biol. 286, 709–720.

Dé, I., Sawicki, S.G., Sawicki, D.L., 1996. Sindbis virus RNA-negative mutants that fail to convert from minus-strand to plus-strand synthesis: role of the nsP2 protein. J. Virol. 70, 2706–2719.

Dreher, T.W., 1999. Functions of the 3′-untranslated regions of positive strand RNA viral genomes. Annu. Rev. Phytopathol. 37, 151–174.

Duggal, R., Lahser, F.C., Hall, T.C., 1994. Cis-acting sequences in the replication of plant viruses with plus-sense RNA genomes. Annu. Rev. Phytopathol. 32, 287–309.

Eckerle, L.D., Ball, L.A., 2002. Replication of the RNA segments of a bipartite viral genome is coordinated by a transactivating subgenomic RNA. Virology 296, 165–176.

Fabian, M.R., Na, H., Ray, D., White, K.A., 2003. 3′-Terminal RNA secondary structures are important for accumulation of Tomato bushy virus DI RNAs. Virology 313, 567–580.

Frolov, I., Hardy, R., Rice, C.M., 2001. Cis-acting RNA elements at the 5′ end of Sindbis virus genome RNA regulate minus- and plus-strand RNA synthesis. RNA 7, 1638–1651.

Guan, H., Song, C., Simon, A.E., 1997. RNA promoters located on (−)-strands of a subviral RNA associated with Turnip crinkle virus. RNA 3, 1401–1412.

Guan, H., Carpenter, C.D., Simon, A.E., 2000. Requirement of a 5′-proximal linear sequence on minus-strand for plus-strand synthesis of a satellite RNA associated with TCV. Virology 268, 355–363.

Herold, J., Andino, R., 2001. Poliovirus RNA replication requires genome circularization through a protein–protein bridge. Mol. Cell 7, 581–591.

Isken, O., Grassmann, C.W., Sarisky, R.T., Kann, M., Zhang, S., Grosse, F., Kao, P.N., Behrens, S.-E., 2003. Members of the NF90/NFAR protein group are involved in the life cycle of a positive-strand RNA virus. EMBO J. 22, 5655–5665.

Kao, C.C., Singh, P., Ecker, D.J., 2001. De novo initiation of viral RNA-dependent RNA synthesis. Virology 287, 251–260.

Khromykh, A.A., Meka, H., Guyatt, K.J., Westaway, E.G., 2001. Essential role of cyclization sequences in flavivirus RNA replication. J. Virol. 75, 6719–6728.

Kim, C.H., Kao, C.C., Tinoco, I., 2000. RNA motifs that determine specificity between a viral replicase and its promoter. Nat. Struct. Biol. 7, 415–423.

Klovins, J., Berzins, V., van Duin, J., 1998. A long-range interaction in Q-beta RNA that bridges the thousand nucleotides between the M-site and the 3′ end is required for replication. RNA 4, 948–957.

Kong, Q., Wang, J., Simon, A.E., 1997. Satellite RNA-mediated resistance to Turnip crinkle virus in Arabidopsis involves a reduction in virus movement. Plant Cell 9, 2051–2063.

McCormack, J., Simon, A.E., 2004. Hypermutability of an RNA virus caused by mutations in an untranslated hairpin. J. Virol. 78, 7813–7817.

Moore, P.B., 1999. Structural motifs in RNA. Annu. Rev. Biochem. 68, 287–300.

Murray, K.E., Steil, B.P., Roberts, A.W., Barton, D.J., 2004. Replication of poliovirus RNA with complete internal ribosome entry site deletions. J. Virol. 78, 1393–1402.

Nagy, P.D., Pogany, J., Simon, A.E., 1999. RNA elements required for RNA recombination function as replication enhancers in vitro and in vivo in a plus-strand RNA virus. EMBO J. 18, 5653–5665.

Nagy, P.D., Pogany, J., Simon, A.E., 2001. In vivo and in vitro characterization of an RNA replication enhancer in a satellite RNA associated with turnip crinkle virus. Virology 288, 315–324.

Panavas, T., Nagy, P.D., 2003. The RNA replication enhancer element of tombusvirus contains two interchangeable hairpins that are functional during plus-strand synthesis. J. Virol. 77, 258–269.

Panavas, T., Pogany, J., Nagy, P.D., 2002. Analysis of minimal promoter sequences for plus-strand synthesis by the Cucumber necrosis virus RNA-dependent RNA polymerase. Virology 296, 263–274.

Pillai-Nair, N., Kim, K.-H., Hemenway, C., 2003. Cis-acting regulatory elements in the Potato virus X 3′ non-translated region differentially affect minus-strand and plus-strand RNA accumulation. J. Mol. Biol. 326, 701–720.

Pogany, J., Fabian, M.R., White, K.A., Nagy, P.D., 2003. Functions of novel replication enhancer and silencer elements in tombusvirus replication. EMBO J. 22, 5602–5611.

Qu, F., Ren, T., Morris, T.J., 2003. The coat protein of Turnip crinkle virus suppresses posttranscriptional gene silencing at an early initiation step. J. Virol. 77, 511–522.

Quadt, R., Ishikawa, M., Janda, M., Ahlquist, P., 1995. Formation of Brome mosaic virus RNA-dependent RNA polymerase in yeast requires coexpression of viral proteins and viral RNA. Proc. Natl. Acad. Sci. U. S. A. 92, 4892–4896.

Ray, D., White, K.A., 1999. Enhancer-like properties of an RNA element that modulates Tombusvirus RNA accumulation. Virology 256, 162–171.

Ray, D., White, K.A., 2003. An internally located RNA hairpin enhances replication of Tomato bushy stunt virus RNAs. J. Virol. 77, 245–257.

Simon, A.E., 2002. The Carmoviruses. The Springer Index of Viruses Online. Springer-Verlag.

Sit, T.L., Vaewhongs, A.A., Lommel, S.A., 1998. RNA-mediated *trans*-activation of transcription from a viral RNA. Science 281, 829–832.

Sivakumaran, K., Kim, C., Tayon Jr., R., Kao, C.C., 1999. RNA sequence and secondary structural determinants in a minimal viral promoter that directs replicase recognition and initiation of genomic plus-strand RNA synthesis. J. Mol. Biol. 294, 667–682.

Song, C., Simon, A.E., 1994. RNA-dependent RNA polymerase from plants infected with turnip crinkle virus can transcribe (+)- and (−)-strands of virus-associated RNAs. Proc. Natl. Acad Sci. U.S.A. 91, 8792–8796.

Song, C., Simon, A.E., 1995. Requirement of a 3′-terminal stem-loop in in vitro transcription by an RNA dependent RNA polymerase. J. Mol. Biol. 254, 6–14.

Sun, X., Simon, A.E., 2003. Fitness of a Turnip crinkle virus satellite RNA correlates with a sequence-nonspecific hairpin and flanking

sequences that enhance replication and repress the accumulation of virions. J. Virol. 77, 7880–7889.

Sun, X., Zhang, G., Simon, A.E., 2004. Short internal sequences involved in RNA replication and virion accumulation in a subviral RNA of Turnip crinkle virus. J. Virol. 79, 512–524.

Thomas, C.L., Leh, V., Lederer, C., Maule, A.J., 2003. Turnip crinkle virus coat protein mediates suppression of RNA silencing in *Nicotiana benthamiana*. Virology 306, 33–41.

Todd, S., Towner, J.S., Brown, D.M., Semler, B.L., 1997. Replication-competent picornaviruses with complete genomic RNA 3′ noncoding region deletions. J. Virol. 71, 8868–8874.

Turner, R.L., Buck, K.W., 1999. Mutational analysis of *cis*-acting sequences in the 3′- and 5′-untranslated regions of RNA2 of Red clover necrotic mosaic virus. Virology 253, 115–224.

van Dijk, A.A., Kakeyev, E.V., Bamford, D.H., 2004. Initiation of viral RNA-dependent RNA polymerization. J. Gen. Virol. 85, 1077–1093.

Vlot, A.C., Neeleman, L., Linthorst, H.J.M., Bol, J.F., 2001. Role of the 3′-untranslated regions of Alfalfa mosaic virus RNA in the formation of a transiently expressed replicase in plants and in the assembly of virions. J. Virol. 75, 6440–6449.

Wang, H.-H., Wong, S.-M., 2004. Significance of the 3′-terminal region in minus-strand RNA synthesis of Hibiscus chlorotic ringspot virus. J. Gen. Virol. 85, 1763–1776.

Wu, B.D., White, K.A., 1998. Formation and amplification of a novel tombusvirus defective RNA which lacks the 5′ nontranslated region of the viral genome. J. Virol. 72, 9897–9905.

You, S., Falgout, B., Markoff, L., Padmanabhan, R., 2001. In vitro RNA synthesis from exogenous Dengue viral RNA templates requires long-range interactions between 5′- and 3′- terminal regions that influence RNA structure. J. Biol. Chem. 276, 15581–15591.

Zhang, F., Simon, A.E., 2003a. Enhanced viral pathogenesis associated with a virulent mutant virus or a virulent satellite RNA correlates with reduced virion accumulation and abundance of free coat protein. Virology 312, 8–13.

Zhang, G., Simon, A.E., 2003b. A multifunctional Turnip crinkle virus replication enhancer revealed by in vivo functional SELEX. J. Mol. Biol. 326, 35–48.

Zhang, G., Zhang, J., Simon, A.E., 2004a. Repression and derepression of minus-strand synthesis in a plus-strand RNA virus replicon. J. Virol. 78, 7619–7633.

Zhang, J., Stuntz, R., Simon, A.E., 2004b. Analysis of a viral replication repressor: sequence requirements in the large symmetrical loop. Virology 326, 90–102.